Excited-State and Photoelectrochemical Behavior of Pyrene-Linked Phenyleneethynylene Oligomer†

Yoichiro Matsunaga,‡,§ Kensuke Takechi,‡ Takeshi Akasaka,§ A. R. Ramesh,|| P. V. James,|| K. George Thomas,|| and Prashant V. Kamat*,‡

Radiation Laboratory, Department of Chemistry and Biochemistry, University of Notre Dame, Notre Dame, Indiana 46556, Center for Tsukuba Advanced Research Alliance, University of Tsukuba, Tsukuba 305-8577, Japan, and Photosciences and Photonics, National Institute for Interdisciplinary Science and Technology (CSIR), Trivandrum 695 019, India

Received: July 03, 2008

An oligophenyleneethynylene (OPE), 1,4-bis(phenyleneethynyl)-2,5-bis(hexyloxy)benzene (**2**), is coupled with pyrene to extend the conjugation and allow its use as a light-harvesting molecule [Py−OPE (**1**)]. The absorption and emission maxima of **1** are red-shifted compared to those of **2**. Similar differences in the singlet and triplet excited-state properties are evident. The fluorescence yield of **2** in toluene is 0.53, which is slightly less than the value for the parent OPE (**2**) of 0.66. The excited singlet and triplet of **1** as characterized from transient absorption spectroscopy exhibit lifetimes of 1.07 ns and 4.0 μs, respectively, in toluene. When **1** was cast as a film on a glass electrode (OTE) and excited with a 387-nm laser pulse, we observed the formation of excitons that decayed within a few picoseconds. When **1** was cast as a film on a SnO_2-modified conducting glass electrode (OTE/SnO_2), a small fraction of excitons dissociated to produce a long-lived charge-separated state. The role of the SnO_2 interface in promoting charge separation was inferred from the photoelectrochemical measurements. Under visible light excitation, the OTE/SnO_2 electrode was capable of generating photocurrent ($\sim$0.25 mA/cm^2) with an incident photon conversion efficiency (IPCE) of $\sim$6%.

Introduction

Conjugated polymers and semiconductor nanostructures are drawing a great deal of attention for the construction of next-generation solar cells.[1] In particular, the versatile optical and semiconducting properties of conjugated polymers and polyelectrolytes have made them useful in solar cells.[2,3] Efficiencies up to 5% have been achieved with polythiophene-based organic solar cells.[4,5] While efforts are being made to investigate the photophysical and charge-carrier-generation properties of these photoactive polymers, oligomeric units provide a convenient way to assess their excited-state properties and factors limiting light energy conversion.

Rigid-rod molecular systems based on phenyleneethynylenes are useful as molecular linkers in optoelectronic devices because of their ability to communicate charge/excitation energy over long distances.[2,6,7] The major advantage of using the oligo(phenyleneethynylene) core unit as a bridge for electronic communication is the cylindrical symmetry of the acetylene unit, which maintains the π-electron conjugation at any degree of rotation.[8] By employing phenyleneethynylene as bridging units, Galoppini and co-workers[8−11] investigated the dynamics of electron injection from excited sensitizers [for example, ruthenium(II) polypyridine and pyrene] to TiO_2 semiconductor. Energy transfer between fullerenes and phenyleneethynylenes has also been studied by synthesizing branched phenyleneethynylene dendrons.[12]

Self-assembly of these oligomers can also be manipulated to obtain interesting nanostructures.[13−15] More recently, Schanze, Reynolds, and co-workers[16,17] have demonstrated the fabrication of photovoltaic cells by layer-by-layer (LBL) assembly using poly(phenyleneethynylene)-based anionic conjugated polyelectrolytes as electron donors. Thus, oligo(*p*-phenyleneethynylene)s (OPEs) have emerged as potential molecular building blocks for the design and fabrication of optoelectronic systems such as solar cells, organic light-emitting diodes (OLEDs), and sensors for the detection of metal ions.

Initial photophysical investigations on phenyleneethynylenes were mainly based on the model system 1,4-bis(phenylethynyl)benzene.[18−21] Recent photophysical and theoretical studies have suggested that phenyleneethynylenes exist in planar and several twisted conformations in their ground state because of the nearly free rotation of the arene rings along the molecular axis.[22,23] In contrast, their emission spectra are highly structured as a consequence of the planarization of the molecules in the excited state.[20−22] Based on picosecond time-resolved resonance Raman spectroscopic investigations, it has also been reported that phenyleneethynylenes exist as a single species in the excited state and that photoexcitation does not bring about any significant changes in the bond order of the acetylene group, ruling out any cumulenic/quinanoidal character in the singlet excited state.[24]

Using transient absorption spectroscopy, we recently characterized the excited states of two model phenyleneethynylenes and concluded that these molecular systems exhibit high excited singlet (0.5−0.7) and triplet (0.3−0.5) yields.[25] Interestingly, this class of molecular systems can transfer energy to a lower-lying triplet (e.g., squaraine dye) or participate in an electron-transfer process (e.g., benzoquinone). Similar energy transfer has also been observed for OPE coupled with a fullerene moiety.[12] Efforts have also been made to characterize photophysical properties of donor−acceptor-based OPE derivatives.[26]

† Part of the "Janos H. Fendler Memorial Issue".

* Address correspondence to this author. E-mail: pkamat@nd.edu.
‡ University of Notre Dame.
§ University of Tsukuba.
|| National Institute for Interdisciplinary Science and Technology (CSIR).

10.1021/jp805878c CCC: $40.75
Published on Web 10/08/2008

CHART 1

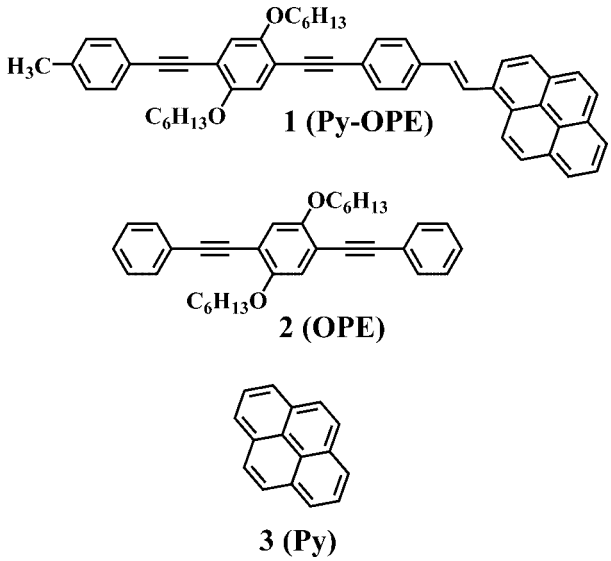

In the present investigation, we have extended the conjugation of the phenyleneethynylene moiety by linking it to a polycyclic aromatic hydrocarbon such as pyrene. By linking a pyrene moiety (**3**) to one of the terminal positions of phenyleneethynylene (Chart 1), we have succeeded in elucidating the excited singlet- and triplet-state behavior and photoelectrochemical properties of a new class of phenyleneethynylene compounds.

Experimental Section

Materials and Methods. The samples (**1** and **2**) used for the study were purified by being passed through a recycling high-performance liquid chromatograph manufactured by Japan Analytical Industry Co., Ltd. All solvents used were of spectrophotometric grade. Absorption spectra were recorded using a Varian model CARY spectrometer. Emission spectra were recorded using an SLM 8000 photon-counting spectrofluorimeter. Emission lifetimes were measured using a Horiba Jobin Vyon single-photon-counting system, and the fluorescence decay measurements were further analyzed using the IBH software library.

Laser Flash Photolysis. Nanosecond laser flash photolysis experiments were performed with a 355-nm laser pulse (5 mJ, pulse width = 6 ns) from a Quanta-Ray Nd:YAG laser system. Femtosecond transient absorption experiments were conducted using a Clark-MXR 2010 laser system and an optical detection system provided by Ultrafast Systems (Helios). The source for the pump and probe pulses was the fundamental of the Clark laser system [775 nm, 1 mJ/pulse (fwhm) 150 fs, 1-kHz repetition rate]. A second-harmonic generator was introduced into the path of the laser beam to provide 387-nm (3.20 eV, 150 fs) laser pulses for the pump. The pump beam was attenuated to 5 μJ/pulse with a spot size of 2 mm (diameter) at the sample where it was merged with the white light incident on the sample cell at an angle of $<10°$. After passing through the 2 mm cell, the probe was focused onto a 200 μm core fiber connected to a CCD spectrograph (Ocean Optics, S2000 UV−vis), enabling time-resolved spectra to be recorded (425−800 nm). Typically, 5000 excitation pulses were averaged to obtain the transient spectrum at a set delay time. Kinetic traces at appropriate wavelengths were assembled from the time-resolved data. All measurements were conducted at room temperature.

Photoelectrochemical Measurements. Photoelectrochemical measurements were performed using a standard three-electrode cell consisting of a dye-deposited OTE working electrode, a saturated calomel electrode (SCE) reference electrode, and a Pt wire gauze counter electrode. Unless otherwise specified, all photoelectrochemical measurements were carried out in water containing 0.5 M NaI and 0.02 mM I_2 at 298 K. Photocurrents at different applied potentials were measured using a Princeton Applied Research model PARSTAT 2263 potentiostat. A 200 W Xe lamp (Oriel) with a copper sulfate filter (>300 nm) was employed as an excitation source. A Bausch and Lomb high-intensity grating monochromator was introduced into the path of the excitation beam for selecting appropriate wavelengths. The incident-photon-to-photocurrent efficiency (IPCE) at various excitation wavelengths was determined from the expression

$$\text{IPCE}\ (\%) = 100 \times \frac{1240 I_{sc}}{I_{inc}\lambda}$$

where I_{sc} is the short-circuit photocurrent (amps per square centimeter), I_{inc} is the incident light intensity (watts per square centimeter), and λ is the wavelength (nanometers). $I-V$ characteristics were recorded by same measurement system under irradiation of white light (100 mW/cm^2) without the monochromator and SCE reference electrode.

Material Synthesis.

Preparation of 5. To a solution of 1-pyrenemethanol **4** (2 g, 8.6 mmol) in dry chloroform (30 mL) was added phosphorus tribromide (2.33 g, 8.6 mmol) dropwise over a period of 30 min under ice-cold conditions. The reaction mixture was stirred at room temperature for 12 h and was neutralized using a saturated solution of sodium bicarbonate. The organic layer was extracted using chloroform, and the solvent was removed under reduced pressure to give **5** (2.5 g, 99%) as a solid; mp 138−140 °C. ^{1}H NMR ($CDCl_3$, 300 MHz) δ: 8.34 (d, 1H, aromatic), 8.18−8.22 (m, 3H, aromatic), 7.90−8.09 (m, 3H, aromatic), 5.2 (s, 2H, CH_2Br). ^{13}C NMR ($CDCl_3$, 75 MHz) δ: 131.89, 131.15, 130.71, 130.51, 129.01 128.17, 127.97, 127.63, 126.21, 125.58, 125.55, 125.05, 124.79, 122.76, 32.13.

Preparation of 6. A mixture of 1-bromomethylpyrene **5** (1 g, 3.4 mmol) and excess triethylphosphite (1 mL) was refluxed for 12 h. The reaction mixture was cooled, and the excess triethylphosphite was removed under reduced pressure to give **6** as a white solid (1.5 g, 78%); mp 130−132 °C. ^{1}H NMR ($CDCl_3$, 300 MHz) δ: 7.9−8.34 (m, 9H, aromatic), 4.11−4.13 (m, 4H, OCH_2), 4.06−4.08 (d, 2H, PCH_2), 1.25−1.36 (m, 6H, alkyl protons). ^{13}C NMR ($CDCl_3$) δ: 131.90, 131.15, 130.71, 130.50, 129.01, 128.17, 127.97, 127.64, 127.27, 126.21, 125.58, 125.55, 125.05, 124.79,124.57, 122.77, 32.13.

Preparation of 8. To a solution of 4-iodotoluene (2 g, 9.17 mmol), CuI (43 mg, 2.5 mmol), and $Pd(PPh_3)_2Cl_2$ (160 mg, 2.5 mmol) in 25 mL of diisopropylamine was added (trimethylsilyl)acetylene (TMSA) (1.3 mL, 9.17 mmol). The mixture was stirred at reflux for 12 h. Solvent was removed, and the crude reaction product was chromatographed over silica gel (100−200 mesh) using hexane as the eluent to yield a light yellow oil (1.3 g, 86%). ^{1}H NMR ($CDCl_3$, 300 MHz) δ: 7.59−6.30 (m, 4H), 2.29 (s, 3H), 0.20 (s, 9H). ^{13}C NMR ($CDCl_3$, 75 MHz) δ: 138.38, 131.78, 128.85, 120.12, 105.41, 93.01, 21.32, 0.032.

Preparation of 9. A mixture of **8** (500 mg, 2.6 mmol), 1,4-bis(hexyloxy)-2,5-diiodobenzene (1.4 g, 2.66 mmol), K_2CO_3 (1.10 g, 7.98 mmol), $Pd(PPh_3)_4$ (154 mg, 0.133 mmol), CuI (25 mg, 0.133 mmol), and triphenylphosphine (139 mg, 0.532 mmol) was stirred at room temperature in a solvent mixture of CH_3OH/THF (1:4) for 15 h. After removal of the solvent under reduced pressure, the crude product was purified by column chromatography over silica gel (100−200 mesh) with hexane/

toluene (1:5) as the eluent to yield **9** (450 mg, 33%); mp 38−40 °C. ^{1}H NMR ($CDCl_3$, 300 MHz) δ: 7.70−6.90 (m, 6H), 3.93 (t, 4H), 2.36 (s, 3H), 1.83−0.86 (m, 22H) ^{13}C NMR ($CDCl_3$, 75 MHz) δ: 154.29, 151.84, 138.38, 131.41, 129.05, 123.93, 120.31, 115.96, 113.93, 94.40, 87.16, 84.86, 70.09, 69.94, 31.56, 31.48, 29.28, 29.14, 25.73, 25.68, 22.59, 21.50, 14.01.

Preparation of 10. To a solution of **9** (400 mg, 0.77 mmol), CuI (15 mg, 0.077 mmol) and $Pd(PPh_3)_2Cl_2$ (27 mg, 0.077 mmol) in 3 mL of diisopropylamine was added TMSA (0.12 mL, 0.85 mmol). The mixture was refluxed for 1 h. Solvent was removed, and the crude reaction product was chromatographed over silica gel (100−200 mesh) using hexane/toluene (1:3) as the eluent to yield **10** as a light yellow solid (240 mg, 63.7%); mp 64−66 °C. ^{1}H NMR ($CDCl_3$, 300 MHz) δ: 7.43−6.94 (m, 6H), 3.98 (t, 4H), 2.36 (s, 3H), 1.85−0.89 (m, 22H), 0.26 (s, 9H). ^{13}C NMR ($CDCl_3$, 75 MHz) δ: 154.17, 153.37, 138.38, 131.44, 129.05, 120.33, 117.33, 116.82, 11.53, 113.41, 101.2, 99.87, 95.09, 85.2, 69.6, 69.46, 31.6, 31.5, 29.29, 25.7, 22.61, 21.5, 14.05, 14.0, −0.057.

Preparation of 11. To a stirred solution of **10** (200 mg, 0.486 mmol) in THF (4 mL) at room temperature were added methanol (1.2 mL) and an aqueous solution of NaOH (0.1 mL, 5 N). The reaction mixture was stirred for 2 h, and the solvent was removed under reduced pressure. The residue obtained was dissolved in chloroform (∼10 mL) and washed with water (2 × 10 mL). The organic layer was dried over anhydrous sodium sulfate. After removal of the solvent, a brown solid (145 mg, 85%) was obtained that was used in a subsequent step without purification; mp 67−69 °C. ^{1}H NMR ($CDCl_3$, 300 MHz) δ: 7.44−6.96 (m, 6H), 3.98 (t, 4H), 3.33 (s, 1H), 2.36 (s, 3H), 1.85−0.89 (m, 22H). ^{13}C NMR ($CDCl_3$, 75 MHz) δ: 154.16, 153.36, 138.45, 131.46, 129.05, 120.27, 117.83, 116.82, 114.94, 112.29, 95.15, 95.09, 82.13, 80.04, 69.66, 69.62, 31.57, 31.51, 29.27, 29.10, 25.7, 25.57, 22.6, 22.56, 21.49, 14.0.

Preparation of 12. To a solution of diisopropylamine (3 mL) in toluene (7 mL) were added **11** (100 mg, 0.24 mmol), 4-bromobenzaldehyde (53 mg, 0.29 mmol), $Pd(PPh_3)_4$ (11 mg, 0.001 mmol), and CuI (1.8 mg, 0.001 mmol). The reaction mixture was refluxed for 24 h, and the solvent was removed under reduced pressure. The product obtained was chromatographed over silica gel (100−200 mesh) using a mixture of toluene/hexane (1:1) as the eluent to give an orange-colored solid (75 mg, 60%); mp 114−116 °C. ^{1}H NMR ($CDCl_3$, 300 MHz) δ: 10.02 (s, 1H), 7.87−7.02 (m, 10H), 2.38 (s, 3H), 1.87−0.90(m, 22H). ^{13}C NMR ($CDCl_3$ 75 MHz) δ: 191.37, 153.92, 153.51, 138.53, 135.29, 132, 131.48, 129.86, 129.54, 129.08, 120.24, 117, 116.74, 115.24, 112.67, 107.56, 106, 95.6, 93.74, 90.32, 85.15, 77.42, 77, 76.57, 69.68, 69.52, 31.58, 29.30, 29.27, 25.72, 22.61, 21.51, 14.0.

Preparation of 1. To a solution of **6** (69 mg, 0.20 mM) in dry THF (15 mL) was added sodium hydride (23 mg, 0.96 mM), and this suspension was added slowly to a solution of **12** (100 mg, 0.19 mmol) in dry THF (3 mL) under argon atmosphere. The mixture was refluxed for 12 h. The solvent was removed under reduced pressure, and the crude product obtained was chromatographed over silica gel (100−200 mesh) using a mixture of toluene/hexane (1:1) as the eluent to give **1** (60 mg, 44%); mp 150−152 °C. ^{1}H NMR ($CDCl_3$) δ: 8.5−7.02 (m, 21H, aromatic), 4.05 (t, 4H, OCH_2), 2.37 (s, 3H), 1.97−0.88 (m, 22H, alkyl protons). ^{13}C NMR ($CDCl_3$ + CS_2, 75 MHz) δ: 153.66, 137.60, 132, 131.60, 131.52, 131.47, 131.03, 129.07, 128.50, 127.71, 127.45, 126.60, 126.46, 126.04, 125.16, 123.63, 12.93, 122.70, 116.90, 113.70, 109.12, 95.18, 25.02, 87.2, 85.32, 77.42, 77, 76.57, 69.65, 59.64, 31.62, 29.33, 25.76, 22.67, 22.64, 21.53, 20.70, 14.09, 14.06.

Results and Discussion

Synthesis of **1** (Py−OPE) was carried out by the condensation reaction of the corresponding aldehyde (**12**) and phosphonate ester (**6**) through a Wittig−Horner reaction (Scheme 1). Details of the synthetic procedure employed for the synthesis of **1** are presented in the Experimental Section. It is important to note that it was somewhat difficult to separate the trace amounts of impurities present in **1** using conventional column chromatographic or crystallization techniques. To ensure high purity of the samples used in the photophysical studies, compounds were further purified using a recycling high-performance liquid chromatograph with two columns connected in series. Typically, 20−30 mg of **1**, dissolved in chloroform (3 mL), was injected and eluted using the same solvent. Effective removal of even trace amounts of impurities could be achieved by recycling the samples for a few cycles. All intermediates and final product were further characterized by various analytical and spectroscopic techniques (Experimental Section). The general strategy employed for the synthesis of compound **2** (OPE) has been reported by our group[22] and others.[27]

Absorption and Emission Characteristics. Phenyleneethynylene oligomers are highly fluorescent ($\Phi_f \approx 0.6$) and absorb strongly in the UV region.[25] The absorption and emission bands shift to longer wavelengths upon extension of the conjugation. Alternatively, it is possible to extend the absorption spectral properties of these oligomers into the visible region through π conjugation with aryl groups.[28] In the present investigation, phenyleneethynylene oligomer (**2**, OPE) was linked to the highly fluorescent molecule pyrene (**3**, Py) to extend its photoresponsive nature. The absorption, emission, and excitation spectra of **1**−**3** in toluene are shown in Figure 1A−C, respectively.

The parent oligo(phenyleneethynylene) (**2**) exhibits absorption in the UV range with a maximum at 367 nm, and pyrene (**3**) exhibits characteristic structured absorption peaks in the UV region (>350 nm). In contrast, the peak of the pyrene−oligo(phenyleneethynylene) adduct (**1**) is rather broad and shifted to the visible region because of the extended conjugation in the coupled system. As shown earlier, extending the π conjugation of the phenyleneethynylene unit with aryl units makes the absorption band shift to the visible range.[17] Thus, in the present case, by linking a pyrene moiety to the phenyleneethynylene unit, we could extend the photoresponsive nature of the latter.

A similar red shift was also seen in the emission spectrum of **1**. The emission of **2** in the range of 450−550 nm comprises two peaks. The peak positions of these two maxima were relatively insensitive to solvent medium. Only about 5 nm shifts in the absorption and emission maxima were seen between nonpolar and polar media. The close matching between the excitation and absorption spectra for each of these compounds (Figure 1) confirmed the singlet excited state of the parent molecule as the origin of the fluorescence. The spectral characteristics of **1** and **2** are compared in Table 1. The singlet excited-state energy of **1** as determined from the crossover point between the normalized absorption and emission spectra was 2.8 eV.

The fluorescence quantum yields were estimated using dilute solutions in different media. The absorbance at the excitation wavelength (355 nm) was maintained at 0.1, and a solution of **2** in toluene was used as the reference ($\Phi = 0.66$).[25] The fluorescence quantum yields of **1** were 0.53 in toluene, 0.59 in

SCHEME 1: Synthetic Route for the Preparation of 1[a]

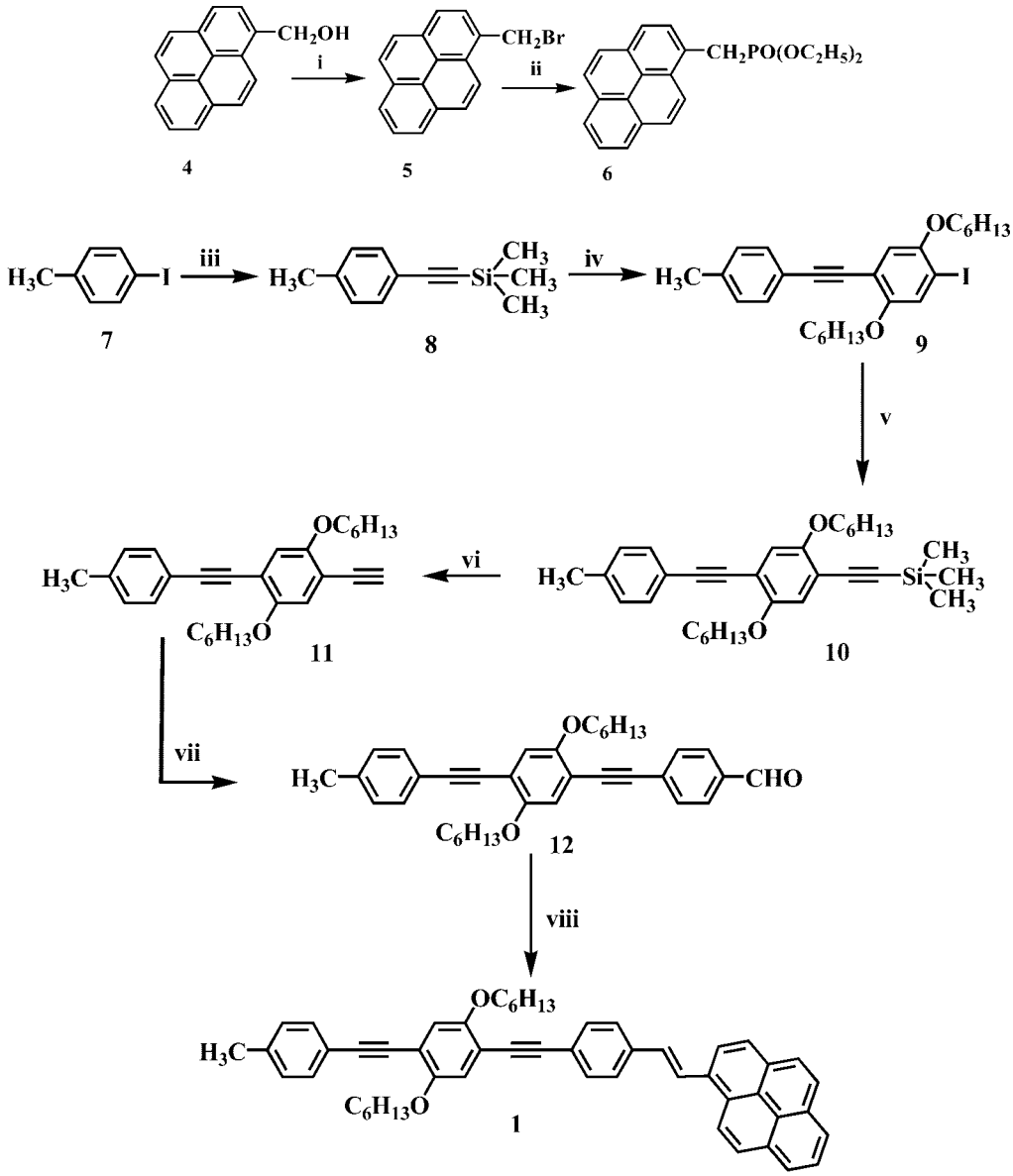

[a] (i) PBr_3, $CHCl_3$; (ii) $P(OEt)_3$; (iii) TMSA, $Pd(PPh_3)_2Cl_2$, CuI, $(i\text{-}Pr)_2NH$; (iv) K_2CO_3, CH_3OH, THF, $Pd(PPh_3)_4$, CuI, 1,4-bis(hexyloxy)-2,5-diiodobenzene; (v) TMSA, $Pd(PPh_3)_2Cl_2$, CuI, $(i\text{-}Pr)_2NH$; (vi) NaOH, CH_3OH, THF; (vii) BrC_6H_4CHO, $(i\text{-}Pr)_2NH$, $Pd(PPh_3)_4$, CuI, toluene; (viii) **6**, NaH, THF.

THF, and 0.61 in CH_2Cl_2 (Table 1). Thus, the quantum yields of **1** obtained from these measurements were close to the values of the parent oligomer, **2**. The photophysical characterization of **1** thus highlights the usefulness of conjugation of the phenyleneethynylene oligomer with pyrene to extend the absorption and emission into the visible region while maintaining a relatively high fluorescence yield.

Singlet Excited State. It is evident from the emission measurements that more than 50% of the singlet excited state decays via radiative decay. The emissions monitored at the respective emission maxima indicate monoexponential decay with lifetimes of 1.07 and 1.43 ns for oligomers **1** and **2**, respectively, in toluene (Figure 2). The inclusion of the pyrene moiety results in slightly shorter excited-singlet lifetimes. Yet, the relatively high quantum yield and the lifetime of ~1 ns indicate that the oligomer **1** retains most of the photophysical characteristics of the parent phenyleneethynylene oligomer **2**. Similar high fluorescence yields have also been reported for pyrene-linked phenylethynyl derivatives.[29]

Duvanel et al.[30] recently investigated the excited-state dynamics of oligomeric phenyleneethynylenes (OPEs) with various lengths and substitutions by femtosecond time-resolved spectroscopy. The decrease in fluorescence lifetime of the OPEs with increasing number of phenyleneethynylene units was attributed to an increase in the oscillator strength for the S_1-S_0 transition. To probe the behavior of the excited singlet state, we performed femtosecond transient absorption spectroscopy measurements. The time-resolved transient absorption spectra recorded following the laser pulse excitation of **1** and **2** are shown in Figure 3. The excited singlet of **2** has a strong absorption in the visible range with a maximum around 590 nm. This transient absorption parallels the bleaching of the ground state at 400 nm. On the other hand, the excited singlet of oligomer **1** exhibits absorption in the IR region with a maximum at 925 nm. It is interesting to note that neither the pyrene (**3**) nor the oligomer **2** exhibits such transient absorption features in the infrared region. The red shift in the singlet−singlet absorption shows that the energy required for the excitation of the S_1 state is significantly decreased for

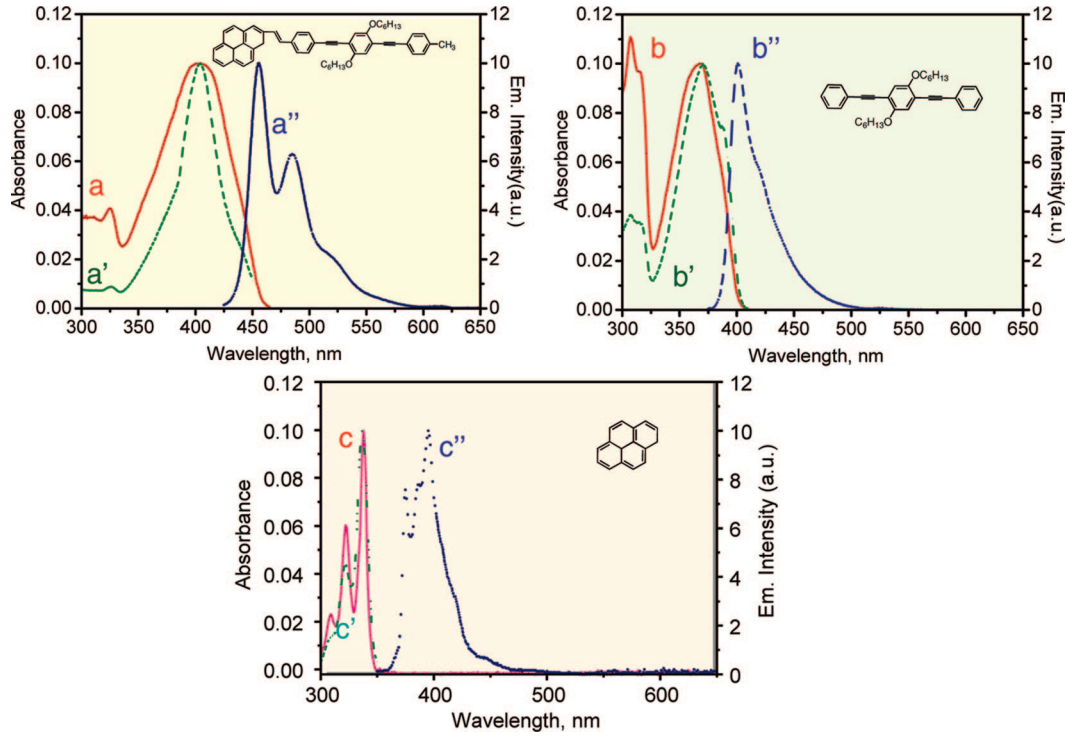

Figure 1. Absorption, excitation, and emission spectra of (A) **1** (a, a′, a″), (B) **2** (b, b′, b″), and (C) **3** (c, c′, c″) recorded in toluene. Excitation spectra (a′, b′, and c′) were recorded using excitation at 457, 401, and 394 nm, respectively. Emission spectra (a″, b″, and c″) were recorded using excitation at 405, 367, and 338 nm, respectively.

TABLE 1: Photophysical Properties of Py−OPE (1) and OPE (2)

oligomer	medium	abs max (nm)	em max (nm)	Φ_f	$\tau_f \pm 0.3$ (ns)	T−T abs max (nm)	$\tau_T \pm 1.0$ (μs)
Py−OPE (**1**)	toluene	405	457,485	0.53	1.07	660	4.0
	THF	409	456,482	0.59	1.23	640	7.0
	CH_2Cl_2	403	457,484	0.61	1.19	640	4.0
	toluene/ethanol[a]	406	460,481	0.54	1.27	640	6.0
OPE (**2**)[b]	toluene	367	401	0.66	1.43	520	14

[a] 1:1 v/v. [b] From ref 25.

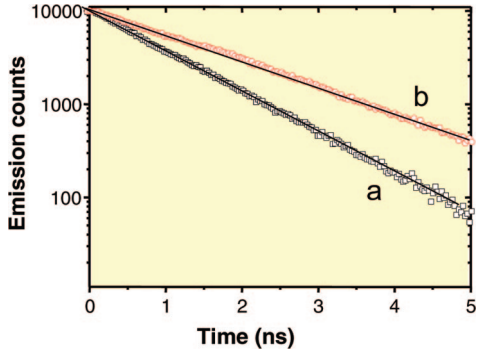

Figure 2. Emission decay of (a) **1** and (b) **2** in toluene probed at 401 and 457 nm, respectively. The excitation wavelength is 373 nm.

2. Thus, extending the conjugation of phenyleneethynylene with a pyrene moiety has a pronounced effect on the S_1-S_n transitions.

The singlet excited state deactivates primarily via intersystem crossing to generate a triplet excited state. The excited singlet-state lifetime measured from the transient decay is similar to the value obtained by fluorescence lifetime measurements (Table 1).

Triplet Excited State. The triplet excited states of **1** and **2** were characterized using 355-nm laser pulse excitation (third harmonic of the Quanta-Ray Nd:YAG laser system). The time-resolved difference absorption spectra are shown in Figure 4. The transient spectrum of **1**, recorded immediately after the laser pulse excitation, shows the formation of a transient with maxima at 660 and 540 nm. The bleaching seen at wavelengths below 400 nm arises from the depletion of the ground state as the oligomers are excited to the triplet state during the 355-nm excitation. The absorption maximum of the triplet excited state of **1** is red-shifted by ~120 nm as compared to that of the triplet excited state of **2**. This shift in the absorption maximum is similar to the shift observed for the singlet excited state. The extended conjugation with the pyrene moiety seems to lower the energy required for the T−T transition.

Excited State Properties of Films. Phenyleneethynylene films exhibit semiconducting properties and have applications in organic light-emitting diodes and organic solar cells. To evaluate the excited-state and photoelectrochemical properties, we cast films of **1** on an optically transparent conducting glass (OTE) and on nanostructured SnO_2 films deposited on OTE (OTE/SnO_2). The absorption and emission spectra are presented in Figure 5. The film of **1** exhibits a broad absorption with a maximum at ~410 nm and an emission maximum at ~510 nm. As compared to the solution spectral features, the major absorption and emission characteristics are retained in the film, except for the broadness of the spectral band. A significant quenching of excited state was noted earlier for pyrene-linked phenyleneethynylene molecules anchored on a TiO_2 surface by

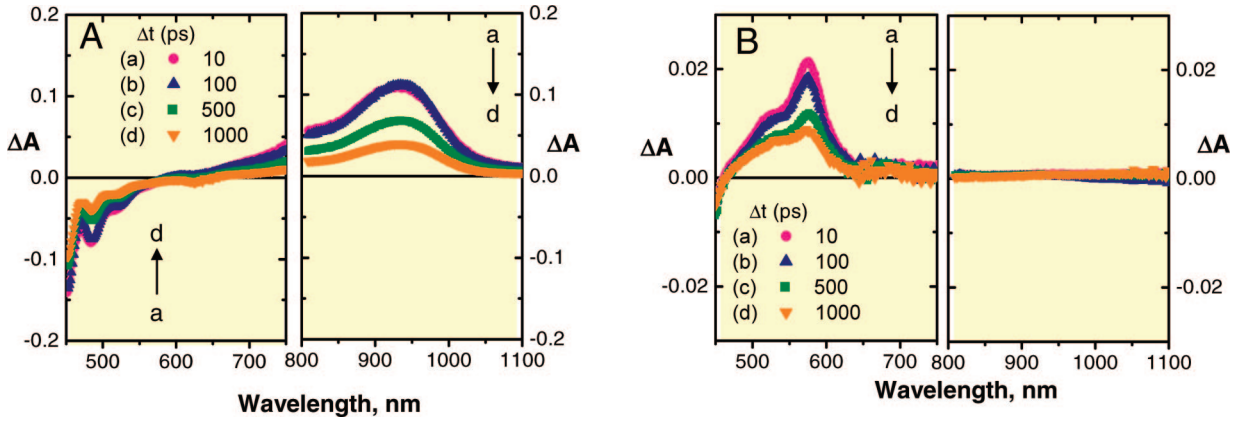

Figure 3. Time-resolved transient absorption spectra of (A) **1** and (B) **2** in toluene at 298 K. The different absorption spectra were recorded (a) 10, (b) 100 (c) 500, and (d) 1000 ps following 387-nm laser pulse excitation. Note that the visible and IR sections of the spectra were collected separately using different detectors.

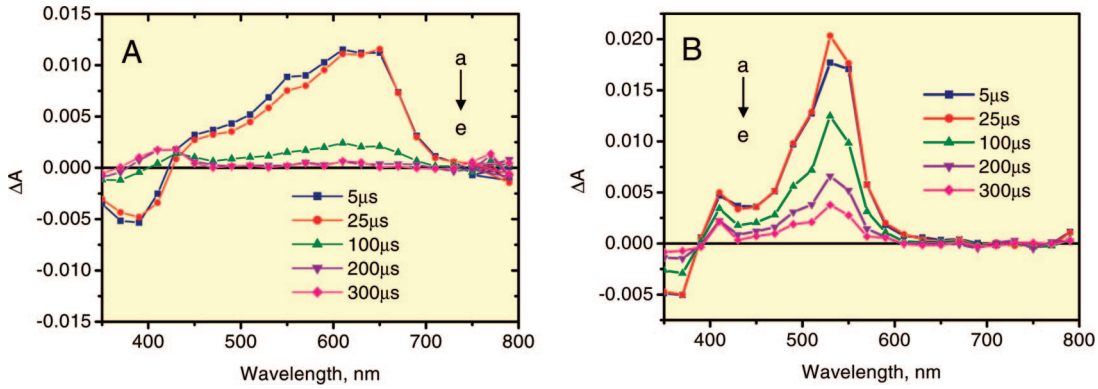

Figure 4. Time-resolved transient absorption spectra of (A) **1** and (B) **2** in toluene at 298 K. The difference absorption spectra were recorded (a) 5, (b) 25, (c) 100, (d) 200, and (e) 300 μs following 355-nm laser pulse excitation.

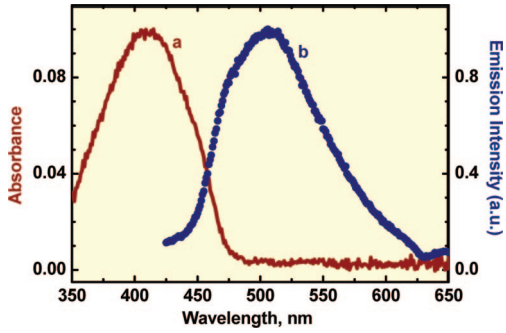

Figure 5. (a) Absorption and (b) emission spectra of **1** cast on an OTE/SnO_2 electrode.

carboxylate linkage.[29] Because the films of **1** cast on OTE and OTE/SnO_2 are multilayer, aggregation and intermolecular interactions are expected to dominate, so that these spectra are broader and the absorption extends further into the visible range.

We also probed the excited-state properties of films of **1** cast on OTE and OTE/SnO_2 electrodes using femtosecond pump−probe spectroscopy. Time-resolved difference absorption spectra recorded after 387-nm laser pulse excitation of **1** cast on OTE/SnO_2 are shown in Figure 6. The transient spectra recorded with the films of **1** on OTE/SnO_2 at early times were similar to those of the film cast on SnO_2. The spectra at these early times (Figure 6) show a broad absorption in the visible and near-IR regions. We attribute this transient absorption arising immediately after laser pulse excitation to the formation of an excitonic state of **1**. The excitons are short-lived as they are susceptible to quick charge recombination. On the OTE electrode, the transient decays quickly without yielding any long-lived products (Figure 7). This fast initial decay (lifetime ≈ 3 ps) is significantly shorter than the singlet lifetime of **1** in solution. This decreased lifetime indicates that the excited-state behavior of **1** in the film is influenced by intermolecular interactions. Similar behavior of the excitonic state has also been noted recently for coronate dye films cast on OTE.[31]

On the other hand, the films of **1** cast on nanostructured SnO_2 films (OTE/SnO_2) exhibit a fast initial decay (lifetime ≈ 3 ps), followed by a long-lived transient that survives over several nanoseconds (Figure 7). We attribute this long-lived transient species to the charge-separated state. As shown in a previous study,[31,32] if the materials are deposited on semiconductor films of SnO_2 and TiO_2, the excitons can undergo charge separation and thus facilitate the formation of a long-lived transient. Comparison of the absorption−time profiles of films of **1** cast on OTE and OTE/SnO_2 confirms the presence of a charge-transfer state. The presence of the SnO_2 film allows the interface to attain a charge-separated state. Indeed, the long-lived charge-transfer state observed in the absorption−time profile (Figure 7) confirms this argument.

Photocurrent Generation of a SnO_2 Electrode Modified with 1. If indeed the SnO_2 interface is responsible for the charge separation in a film of **1**, one should be able to collect the charge carriers in a photoelectrochemical cell. A photoelectrochemical cell was constructed using the oligomer films (**1** and **2**) cast on an OTE/SnO_2 electrode surface as the photoanodes. Figure 8 shows the photocurrent and photovoltage responses to visible light. The generation of photocurrent and photovoltage was prompt, steady, and reproducible during several on/off cycles

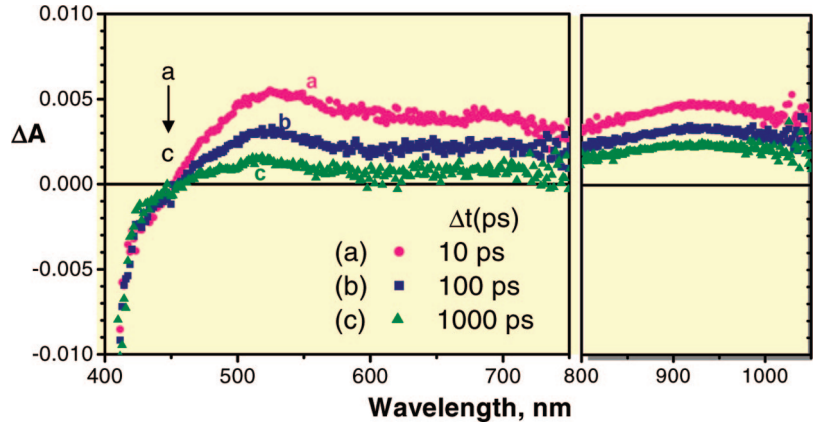

Figure 6. Transient absorption spectra recorded following 387-nm laser pulse excitation of a film of **1** cast on nanostructured SnO_2 film (OTE/SnO_2).

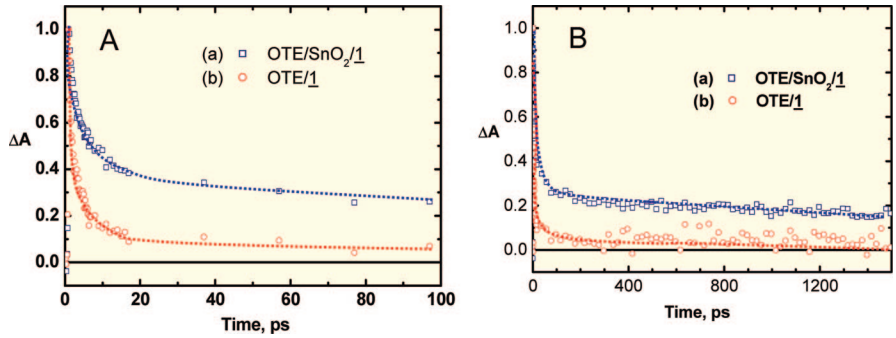

Figure 7. Absorption−time profiles recorded at 930 nm for the (A) short and (B) long time scales following 387-nm laser pulse excitation of (a) OTE/SnO_2/**1** and (b) OTE/**1**. Note that the presence of a long-lived transient is observed only when the film is cast on the SnO_2 surface.

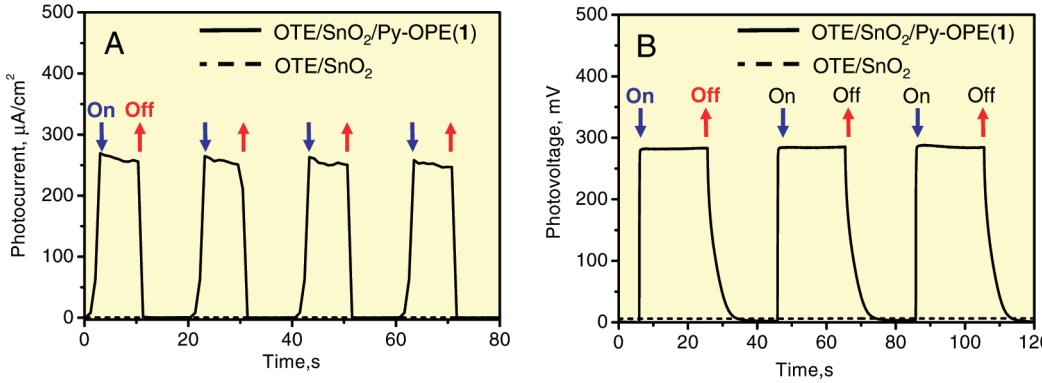

Figure 8. (A) Photocurrent and (B) photovoltage responses of OTE/SnO_2/**1** electrode to visible light illumination (λ > 350 nm) (electrolyte, 0.5 M NaI and 0.02 mM I_2 in water; input power, 100 mW/cm^2).

of white light (λ > 370 nm, 100 mW/cm^2) illumination. As the OTE/SnO_2/**1** electrode is excited with visible light, a fraction of the excitons generated at the SnO_2 interface undergo charge separation. As the electrons are collected by the SnO_2, the holes are scavenged by the I_3^-/I^- redox couple present in the electrolyte.

Figure 9A shows the photocurrent action spectrum of the OTE/SnO_2/**1** electrode presented in terms of incident-photon-to-charge-carrier generation efficiency (IPCE) versus wavelength of excitation. The experiments were carried out in a two-arm flat cell using monochromatic light and the illumination was limited to an electrode area of 0.32 cm^2. The OTE/SnO_2/**1** electrode shows a photocurrent response at wavelengths below 480 nm with a maximum IPCE value of around 6%. Comparison with the absorption spectrum of the film of **1** shows that the origin of the photocurrent corresponds to the excitation of **1**. Although we were not able to harvest most of the visible photons, the extended conjugation with the pyrene moiety is useful in making the phenyleneethynylene oligomers responsive to visible light (up to 480 nm). The IPCE value is nearly an order of magnitude greater than that reported for TiO_2 films with monolayer coverage.[29] More recently, an IPCE of 11% has been achieved using a polymeric system, viz., poly(*p*-phenyleneethynylene) on TiO_2 electrodes. [16] The spectral response was further broadened in this case through the incorporation of carboxylated polythiophene derivative.

Figure 9B shows the power characteristics of the photoelectrochemical cell constructed with OTE/SnO_2/**1**. A stable photocurrent of 0.25 mA/cm^2 and an open-circuit voltage of 300 mV were observed under visible light irradiation of 100 mW/cm^2.

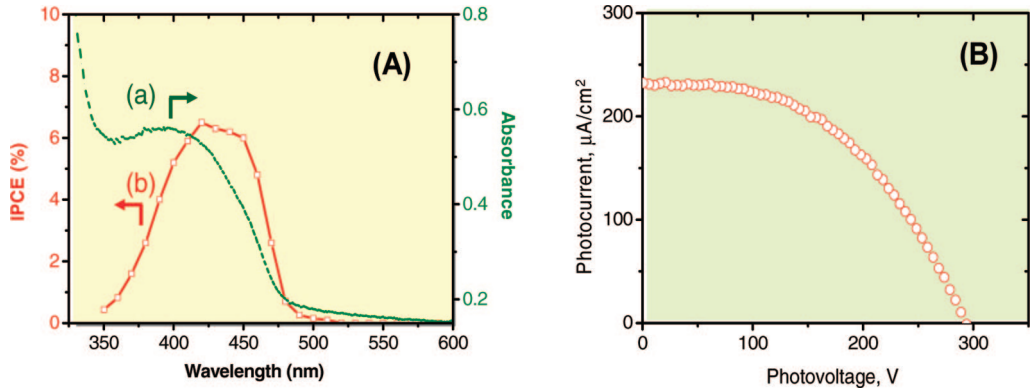

Figure 9. (A) (a) Absorption spectrum and (b) photocurrent action spectrum of OTE/SnO_2/**1**. (B) $I-V$ characteristics of OTE/SnO_2/**1** electrode under white light (λ > 350 nm, input power 100 mW/cm^2) illumination. (Electrolyte: 0.5 M NaI and 0.02 mM I_2 in water.)

The overall power conversion efficiency of the cell was ~0.05%. This low power conversion efficiency is indicative of the fact that the photon-to-charge-carrier generation is rather poor. As shown in our transient absorption studies, only a small fraction of the excitons are able to dissociate at the SnO_2 interface. The electron transport across the SnO_2 network also remains a bottleneck for charge transport. One way to facilitate charge transport is to introduce the conducting scaffold of a single-walled carbon nanotube (SWCNT). Preliminary studies have indicated that SWCNT/semiconductor nanostructure assemblies are useful in improving the efficiency of light-harvesting assemblies. Another approach is to broaden the spectral response by incorporating a second light-harvesting component. In a recent study, a similar approach was undertaken by incorporating carboxylated polythiophene derivative along with poly(*p*-phenyleneethynylene) on TiO_2 electrodes. Further efforts are underway to utilize this strategy in improving the photoconversion efficiency of phenyleneethynylene-based organic solar energy systems.

Conclusions

The absorption range of 1,4-bis(phenyleneethynyl)-2,5-bis(hexyloxy)benzene has been extended into the visible range by linking it to a pyrene unit. Extension of the π conjugation allowed for the modification of the excited-state properties of the phenylethynelene oligomer. The ability of the Py−OPE film to undergo charge separation at the SnO_2 interface can be utilized for the photocurrent generation. The observed IPCE of 6% highlights the potential application of such conjugated oligomers for the development of inorganic−organic hybrid systems for photochemical solar cells.

Acknowledgment. P.V.K. and Y.M. acknowledge support from the Office of Basic Energy Science of the U.S. Department of the Energy. Y.M. also acknowledges the support of JSPS for allowing the opportunity to conduct research at Notre Dame. We also thank Toyota Central R&D Laboratories., Inc., Aichi, Japan, for the research grant enabling T.K. to stay at Notre Dame. K.G.T., A.R.R., and P.V.J. thank the Department of Science and Technology, Government of India, for financial support. This is contribution no. NDRL 4768 from the Notre Dame Radiation Laboratory and contribution no. PPD 271 from the Photosciences and Photonics of the National Institute for Interdisciplinary Science and Technology.

References and Notes

(1) Kamat, P. V. Meeting the Clean Energy Demand: Nanostructure Architectures for Solar Energy Conversion. *J. Phys. Chem. C* **2007**, *111*, 2834–2860.

(2) Silverman, E. E.; Cardolaccia, T.; Zhao, X. M.; Kim, K. Y.; Haskins-Glusac, K.; Schanze, K. S. The triplet state in Pt-acetylide oligomers, polymers and copolymers. *Coord. Chem. Rev.* **2005**, *249*, 1491–1500.

(3) Pingree, L. S. C.; MacLeod, B. A.; Ginger, D. S. The changing face of PEDOT:PSS films: Substrate, bias, and processing effects on vertical charge transport. *J. Phys. Chem. C* **2008**, *112*, 7922–7927.

(4) Campoy-Quiles, M.; Ferenczi, T.; Agostinelli, T.; Etchegoin, P. G.; Kim, Y.; Anthopoulos, T. D.; Stavrinou, P. N.; Bradley, D. D. C.; Nelson, J. Morphology evolution via self-organization and lateral and vertical diffusion in polymer: fullerene solar cell blends. *Nat. Mater.* **2008**, *7*, 158–164.

(5) Quist, P. A. C.; Sweelssen, J.; Koetse, M. M.; Savenije, T. J.; Siebbeles, L. D. A. Formation and decay of charge carriers in bulk heterojunctions of MDMO−PPV or P3HT with new *n*-type conjugated polymers. *J. Phys. Chem. C* **2007**, *111*, 4452–4457.

(6) Pinto, M. R.; Schanze, K. S. Conjugated polyelectrolytes: Synthesis and applications. *Synthesis* **2002**, 1293–1309.

(7) Wong, W. Y. Luminescent organometallic poly(aryleneethynylene)s: functional properties towards implications in molecular optoelectronics. *Dalton Trans.* **2007**, 4495–4510.

(8) Galoppini, E. Linkers for anchoring sensitizers to semiconductor nanoparticles. *Coord. Chem. Rev.* **2004**, *248*, 1283–1297.

(9) Hoertz, P. G.; Carlisle, R. A.; Meyer, G. J.; Wang, D.; Piotrowiak, P.; Galoppini, E. Organic rigid-rod linkers for coupling chromophores to metal oxide nanoparticles. *Nano Lett.* **2003**, *3*, 325–330.

(10) Wang, D.; Mendelsohn, R.; Galoppini, E.; Hoertz, P. G.; Carlisle, R. A.; Meyer, G. J. Excited state electron transfer from Ru(II) polypyridyl complexes anchored to nanocrystalline TiO_2 through rigid-rod linkers. *J. Phys. Chem. B* **2004**, *108*, 16642–16653.

(11) Myahkostupov, M.; Piotrowiak, P.; Wang, D.; Galoppini, E. Ru(II)-Bpy complexes bound to nanocrystalline TiO_2 films through phenyleneethynylene (OPE) linkers: Effect of the linkers length on electron injection rates. *J. Phys. Chem. C* **2007**, *111*, 2827–2829.

(12) Clifford, J. N.; Gegout, A.; Zhang, S.; De Freitas, R. P.; Urbani, M.; Holler, M.; Ceroni, P.; Nierengarten, J. F.; Armaroli, N. Fullerene derivatives substituted with differently branched phenyleneethynylene dendrons: Synthesis, electronic and excited state properties. *Eur. J. Org. Chem.* **2007**, 5899–5908.

(13) Wackerly, J. W.; Moore, J. S. Cooperative self-assembly of oligo(m-phenyleneethynylenes) into supramolecular coordination polymers. *Macromolecules* **2006**, *39*, 7269–7276.

(14) Nilsson, D.; Watcharinyanon, S.; Eng, M.; Li, L. Q.; Moons, E.; Johansson, L. S. O.; Zharnikov, M.; Shaporenko, A.; Albinsson, B.; Martensson, J. Characterization of self-assembled monolayers of oligo(phenyleneethynylene) derivatives of varying shapes on gold: Effect of laterally extended π-systems. *Langmuir* **2007**, *23*, 6170–6181.

(15) Yoosaf, K.; James, P. V.; Ramesh, A. R.; Suresh, C. H.; Thomas, K. G. Self-organization of phenyleneethynylene into wire-like molecular materials on surfaces. *J. Phys. Chem. C* **2007**, *111*, 14933–14936.

(16) Mwaura, J. K.; Zhao, X.; Jiang, H.; Schanze, K. S.; Reynolds, J. R. Spectral Broadening in Nanocrystalline TiO_2 Solar Cells Based on Poly(*p*-phenylene ethynylene) and Polythiophene Sensitizers. *Chem. Mater.* **2006**, *18*, 6109–6111.

(17) Mwaura, J. K.; Pinto, M. R.; Witker, D.; Ananthakrishnan, N.; Schanze, K. S.; Reynolds, J. R. Photovoltaic Cells Based on Sequentially Adsorbed Multilayers of Conjugated Poly(*p*-phenylene ethynylene)s and a Water-Soluble Fullerene Derivative. *Langmuir* **2005**, *21*, 10119–10126.

(18) Levitus, M.; Schmieder, K.; Ricks, H.; Shimizu, K. D.; Bunz, U. H. F.; Garcia-Garibay, M. A. Steps to demarcate the effects of chromophore aggregation and planarization in poly(phenyleneethynylene)s. 1. Rotationally interrupted conjugation in the excited states of 1,4-bis(phenylethynyl)benzene. *J. Am. Chem. Soc.* **2001**, *123*, 4259–4265.

(19) Li, H.; Powell, D. R.; Firman, T. K.; West, R. Structures and photophysical properties of model compounds for arylethylene disilylene polymers. *Macromolecules* **1998**, *31*, 1093–1098.

(20) Beeby, A.; Findlay, K.; Low, P. J.; Marder, T. B. A re-evaluation of the photophysical properties of 1,4-bis(phenylethynyl)benzene: A model for poly(phenyleneethynylene). *J. Am. Chem. Soc.* **2002**, *124*, 8280–8284.

(21) Zhao, L.; Perepichka, I. F.; Turksoy, F.; Batsanov, A. S.; Beeby, A.; Findlay, K. S; Bryce, M. R. 2,5-Di(aryleneethynyl)pyrazine derivatives: Synthesis, structural and optoelectronic properties, and light-emitting device. *New J. Chem.* **2004**, *28*, 912–918.

(22) James, P. V.; Sudeep, P. K.; Suresh, C. H.; Thomas, K. G. Photophysical and theoretical investigations of oligo(*p*-phenyleneethynylene)s: Effect of alkoxy substitution and alkyne−aryl bond rotations. *J. Phys. Chem. A* **2006**, *110*, 4329–4337.

(23) Liu, L. T.; Yaron, D.; Berg, M. A. Electron−phonon coupling in phenyleneethynylene oligomers: A nonlinear one-dimensional configuration-coordinate model. *J. Phys. Chem. C* **2007**, *111*, 5770–5782.

(24) Beeby, A.; Findlay, K. S.; Low, P. J.; Marder, T. B.; Matousek, P.; Parker, A. W.; Rutter, S. R.; Towrie, M. Studies of the S1 state in a prototypical molecular wire using picosecond time-resolved spectroscopies. *Chem. Commun.* **2003**, 2406–2407.

(25) Sudeep, P. K.; James, P. V.; Thomas, K. G.; Kamat, P. V. Singlet and Triplet Excited State Interactions and Photochemical Reactivity of Phenyleneethynylene Oligomers. *J. Phys. Chem. A* **2006**, *110*, 5642–5649.

(26) Yamaguchi, Y.; Shimoi, Y.; Ochi, T.; Wakamiya, T.; Matsubara, Y.; Yoshida, Z. I. Photophysical properties of oligophenylene ethynylenes modified by donor and/or acceptor groups. *J. Phys. Chem. A* **2008**, *112*, 5074–5084.

(27) Li, H.; Powell, D. R.; Hayashi, R. K.; West, R. Poly((2,5-dialkoxy-*p*-phenylene)ethynylene-*p*-phenyleneethynylene)s and Their Model Compounds. *Macromolecules* **1998**, *31*, 52–58.

(28) Zhao, X.; Pinto, M. R.; Hardison, L. M.; Mwaura, J.; Muller, J.; Jiang, H.; Witker, D.; Kleiman, V. D.; Reynolds, J. R.; Schanze, K. S. Variable Band Gap Poly(arylene ethynylene) Conjugated Polyelectrolytes. *Macromolecules* **2006**, *39*, 6355–6366.

(29) Taratula, O.; Rochford, J.; Piotrowiak, P.; Galoppini, E.; Carlisle, R. A.; Meyer, G. J. Pyrene-terminated phenylenethynylene rigid linkers anchored to metal oxide nanoparticles. *J. Phys. Chem. B* **2006**, *110*, 15734–15741.

(30) Duvanel, G.; Grilj, J.; Schuwey, A.; Gossauer, A.; Vauthey, E. Ultrafast excited-state dynamics of phenyleneethynylene oligomers in solution. *Photochem. Photobiol. Sci.* **2007**, *6*, 956–963.

(31) Takechi, K.; Kamat, P. V.; Avira, R. R.; Jyothi, K.; Ramaih, D. Harvesting Infrared Photons with Croconate Dyes. *Chem. Mater.* **2008**, *20*, 265–272.

(32) Takechi, K.; Sudeep, S; Kamat, P. V. Harvesting Infrared Photons with Tricarbocyanine Dye Clusters. *J. Phys. Chem. B* **2006**, *110*, 16169–16173.

JP805878C